

# Acceleration of Metal Nanoparticle with Irradiation Pressure

Nicolas I. Grigorchuk \*

*Bogolyubov Institute for Theoretical Physics, National Academy of Sciences of Ukraine,  
14-b Metrologichna Str., Kyiv-143, Ukraine, 03143*

The acceleration of an spheroidal metal nanoparticle in an irradiation field with a frequency close to the surface plasmon vibration has been considered. Under the action of radiation pressure, the polarizability for nonspherical particle becomes a tensor quantity. The analytical expressions for the resonance acceleration components for the cases of plane-polarized and circularly polarized light have been derived. We have demonstrated that the resonance acceleration can depend substantially on the shape of a metal nanoparticle and its orientation with respect to the directions of light propagation and the light polarization.

PACS numbers: PACS numbers: 41.75.Jv; 42.50.Wk; 78.67.Bf

## I. INTRODUCTION

The advent of lasers made the development of researches in the field of microparticle trapping, confinement, and manipulation possible<sup>1</sup>. The hot-electron pressure triggers the anisotropic shape oscillations due to the thermal expansion of the optically heated particles<sup>2</sup>. The resonant radiation pressure on neutral particles was investigated in<sup>3</sup>. Rawson and May observed the angular stabilization of matter by radiation<sup>4</sup> which is familiar to trapping of small particles by radiation pressure. In 1970, Arthur Ashkin<sup>5</sup> has been demonstrated, for the first time, the trapping and the manipulating of a micron-sized dielectric spherical particle in the field of two opposing laser beams. An another work<sup>6</sup> was devoted to the observation of resonances in the radiation pressure on dielectric spheres. The plasmon-resonance conditions for optical forces on small particles was than considered in detail by Arias-González and Nieto-Vesperinas<sup>7</sup>. More latter it was developed the theory of optical tweezers<sup>8</sup>. Much efforts to develop the photonic force spectroscopy on metal nanoparticles (MNs) was applied by P. Chaument with coauthors<sup>9</sup>.

For recent years, intensively developed have been both the researches of the peculiarities inherent to the mechanisms of light pressure action upon nanoparticles and the implication of this action in the tasks of small particle manipulation. Such applications meet a wide usage in biology, medicine, and microelectronics.

A theory for the generation in a spheroidal MN of an angular momentum under the action of ultrashort laser pulse is developed in the work<sup>10</sup>. The optical radiation force on a dielectric sphere illuminated by a linearly polarized Airy light-sheet was studied recently in<sup>11</sup>. A review of some relevant problems can be found, e.g., in the work<sup>12</sup>.

A theoretical study of the time-averaged force exerting upon a spherical particle in a time-harmonic-varying

electromagnetic field has been carried out in the work<sup>7</sup>. The expression obtained there for the force components depends on the gradient of the electromagnetic wave intensity and on the particle's polarizability. The particle was considered spherical, so that its polarizability was characterized by a scalar parameter.

In present work, we consider MNs of the spheroidal form. In this case, the particle polarizability becomes a tensor and can depend rather strongly on the particle's morphology<sup>13</sup>. Moreover, the high-frequency (optical) conductivity<sup>14</sup>, which is connected to the imaginary part of particle's polarizability and defines its absorption, also becomes a tensor. The dependence of the polarizability of MN on its form becomes especially appreciable in the infra-red range of frequencies. As a result, the expression for the components of the MN acceleration with action of the laser beam, would differ substantially from those obtained in the spherical case.

## II. FORMULATION OF THE PROBLEM

For particles, whose dimensions are considerably smaller than the length of the electromagnetic wave, we apply the Rayleigh approximation, i.e. the particle is considered as a dipole in a non-uniform field. The force affecting such a particle equals

$$\mathbf{F} = (\mathbf{P} \cdot \nabla) \mathbf{E} + \frac{1}{c} \dot{\mathbf{P}} \times \mathbf{B}, \quad (1)$$

where  $\mathbf{P}$  is the dipole moment of the particle,  $\mathbf{E}$  the electric and  $\mathbf{B}$  the magnetic fields, and  $c$  the speed of light. All quantities in Eq. (1) are real. For our purpose, it is convenient to use the complex ones, using in Eq. (1) for an arbitrary vector ( $\mathbf{V}$ ) the conditional scheme

$$\mathbf{V} \Rightarrow \frac{1}{2}(\mathbf{V} + \mathbf{V}^*). \quad (2)$$

We will suppose that the complex quantities are depended on time harmonically:

$$\mathbf{V}^* = \mathbf{V}_0 \exp(-i\omega t). \quad (3)$$

\*email: ngrigor@bitp.kiev.ua

Here  $\omega$  is the frequency of the electromagnetic wave. Now, we can introduce the electromagnetic acceleration averaged over the time period  $T$ :

$$\begin{aligned} \bar{\mathbf{A}} &= \frac{1}{4TM} \int_{-T/2}^{T/2} dt \left\{ [(\mathbf{P} + \mathbf{P}^*) \cdot \nabla](\mathbf{E} + \mathbf{E}^*) \right. \\ &\quad \left. \times \frac{1}{c} (\dot{\mathbf{P}} + \dot{\mathbf{P}}^*) \times (\mathbf{B} + \mathbf{B}^*) \right\}, \end{aligned} \quad (4)$$

where  $M$  is the mass of the particle. The second term in the integrand of expression (4) can be integrated by parts with using well-known ratio

$$-\frac{1}{c} \frac{d\mathbf{B}}{dt} = \text{rot } \mathbf{E}. \quad (5)$$

Then, instead of Eq. (4), we obtain

$$\begin{aligned} \bar{\mathbf{A}} &= \frac{1}{4MT} \int_{-T/2}^{T/2} dt \left\{ ((\mathbf{P} + \mathbf{P}^*) \cdot \nabla)(\mathbf{E} + \mathbf{E}^*) \right. \\ &\quad \left. + \frac{1}{c} (\mathbf{P} + \mathbf{P}^*) \times [\nabla \times (\mathbf{E} + \mathbf{E}^*)] \right\}. \end{aligned} \quad (6)$$

Now, taking advantage of the explicit dependence on time (see Eqs. (3)), it is easy to carry out the integration in Eq. (6) in time. The acceleration averaged over wave period which is connected with the dipole moment  $P_0$  in the general case will have the form

$$\begin{aligned} \bar{\mathbf{A}} &= \frac{1}{4M} \left\{ (\mathbf{P}_0 \cdot \nabla) \mathbf{E}_0^* + (\mathbf{P}_0^* \cdot \nabla) \mathbf{E}_0 \right. \\ &\quad \left. + \mathbf{P}_0 \times [\nabla \times \mathbf{E}_0^*] + \mathbf{P}_0^* \times [\nabla \times \mathbf{E}_0] \right\}. \end{aligned} \quad (7)$$

Later we will use formula (7) to calculate the MN acceleration under resonant irradiation by the laser beam.

Below, we consider a MN with an ellipsoid-of-revolution form. In the reference frame connected to the principal axes of this ellipsoid, the dipole moment of such a particle looks like<sup>15</sup>

$$P_{0j} = \frac{V}{4\pi} \frac{\varepsilon_{jj} - 1}{1 + L_j(\varepsilon_{jj} - 1)} E_{0j}, \quad j = x, y, z. \quad (8)$$

Here,  $V$  is the volume of the MN,  $L_j$  are the depolarization factors,

$$\varepsilon_{jj} = \varepsilon'_{jj} + \varepsilon'' = \varepsilon' + i \frac{4\pi}{\omega} \sigma_{jj}, \quad (9)$$

$\varepsilon'$  is the real part of the dielectric constant which has the form

$$\varepsilon' = 1 - \frac{\omega_{pl}^2}{\omega^2}, \quad (10)$$

$\omega_{pl}$  is the plasma oscillation frequency, and  $\sigma_{jj}$  are the diagonal elements of the tensor of high-frequency (optical) conductivity.

We admit the characteristic particle sizes are smaller than the mean free path of an electron in the direction of its scattering by phonons. Provided both such sizes and the asymmetric form of the MN, the conductivity becomes a tensor value as was demonstrated in work<sup>16</sup>. In turn, the conductivity and, therefore, dissipation are due to the action of both the electric field  $E$  (electric absorption) and the magnetic field  $B$  (magnetic absorption) of the electromagnetic wave. In the case of MN with the form of an ellipsoid of revolution, the following components of the tensor  $\sigma_{jj}$  are distinct from zero in the reference frame connected to the principal axes of this ellipsoid:

$$\sigma_{xx} = \sigma_{yy} \equiv \sigma_{\perp}, \quad \sigma_{zz} \equiv \sigma_{\parallel}, \quad (11)$$

while the depolarization factors equal

$$L_x(e_p) = L_y(e_p) = \frac{1}{2}[1 - L_z(e_p)] \equiv L_{\perp}, \quad (12)$$

$$L_z(e_p) \equiv L_{\parallel} = \begin{cases} \frac{1 - e_p^2}{2e_p^3} \left( \ln \frac{1 + e_p}{1 - e_p} - 2e_p \right), & R_{\perp} < R_{\parallel} \\ \frac{1 + e_p^2}{e_p^3} (e_p - \arctan e_p), & R_{\perp} > R_{\parallel} \end{cases}. \quad (13)$$

In expressions (13) the notation

$$e_p^2 = \begin{cases} 1 - R_{\perp}^2/R_{\parallel}^2, & R_{\perp} < R_{\parallel} \\ R_{\perp}^2/R_{\parallel}^2 - 1, & R_{\perp} > R_{\parallel} \end{cases}, \quad (14)$$

is used, where  $R_{\parallel}$  and  $R_{\perp}$  are the corresponding semi-axes of the ellipsoid of revolution ( $R_{\parallel}$  is along with revolution axis and  $R_{\perp}$  is perpendicular to this axis).

Introducing the vector components of the dipole moment in the form

$$P_{0i} = \sum_j \alpha_{ij} E_{0j}, \quad (15)$$

Eqs. (8) and (11) yield the following expressions for nonzero components of the polarizability tensor  $\alpha_{jj}$ :

$$\alpha_{xx} = \alpha_{yy} \equiv \alpha_{\perp} = \frac{V}{4\pi} \frac{(\varepsilon_{\perp} - 1)}{1 + L_{\perp}(\varepsilon_{\perp} - 1)}, \quad (16)$$

$$\alpha_{zz} \equiv \alpha_{\parallel} = \frac{V}{4\pi} \frac{(\varepsilon_{\parallel} - 1)}{1 + L_{\parallel}(\varepsilon_{\parallel} - 1)}, \quad (17)$$

where

$$\varepsilon_{\parallel} = \varepsilon' + i \frac{4\pi}{\omega} \sigma_{\parallel}, \quad \varepsilon_{\perp} = \varepsilon' + i \frac{4\pi}{\omega} \sigma_{\perp}. \quad (18)$$

The expressions for  $\sigma_{\perp}$  and  $\sigma_{\parallel}$  for various specific conditions are presented in the work<sup>13</sup>. In particular, if the electric absorption dominates, simple analytical expressions for the components  $\sigma_{\perp}$  and  $\sigma_{\parallel}$  can be obtained in

the cases of strongly prolate ( $R_{\parallel} \gg R_{\perp}$ ) and strongly oblate ( $R_{\parallel} \ll R_{\perp}$ ) ellipsoids<sup>13</sup>:

$$\sigma_{\parallel} \approx \frac{3}{2}\sigma_{\perp} \approx \frac{9\pi}{64} \frac{v_F}{R_{\perp}} \frac{ne^2}{m\omega^2} \quad (R_{\parallel} \gg R_{\perp}), \quad (19)$$

$$\sigma_{\parallel} \approx \frac{1}{2}\sigma_{\perp} \approx \frac{9}{16} \frac{v_F}{R_{\parallel}} \frac{ne^2}{m\omega^2} \quad (R_{\parallel} \ll R_{\perp}). \quad (20)$$

Here,  $v_F$  is the Fermi velocity,  $n$  the concentration of electrons, and  $m$  the electron mass.

For spherical MNs ( $R_{\parallel} = R_{\perp} = R$ ), we obtain

$$\sigma_{\parallel} = \sigma_{\perp} = \frac{3}{4} \frac{v_F}{R} \frac{ne^2}{m\omega^2}. \quad (21)$$

Formulae (19) and (20) are valid in the case of high-frequency fields, when the frequency of light is higher than the transit-time ones ( $\omega > v_F/R_{\perp}, v_F/R_{\parallel}$ ).

Starting from formula (15) with using Eq. (11), the dipole moment can be written down for arbitrary coordinate system in the form

$$\mathbf{P}_0 = \alpha_{\perp} \mathbf{E}_0 + (\alpha_{\perp} - \alpha_{\parallel})(\mathbf{nE}_0)\mathbf{n}. \quad (22)$$

Here,  $\mathbf{n}$  is a unit vector directed along the axis of rotation of the ellipsoid. Formulae (22) and (7) will serve as the basic ones for studying the MN acceleration.

### III. ACCELERATION UNDER THE ACTION OF LIGHT PRESSURE

In order to obtain the explicit expression for the time-averaged acceleration (7), it is necessary to establish the

coordinate dependence of the field  $\mathbf{E}_0$ . As the first example of such a dependence, we take this field in the form with a linear polarization along  $x$ -axis. It looks like

$$\mathbf{E}_0 = (E_x, 0, 0); \quad E_x = E_0 e^{-x^2/(2a^2)} e^{ikz}, \quad (23)$$

where  $a$  is the radius of the light beam. Substituting expressions (22) and (23) into Eqs. (7), we obtain the expressions for nonzero components of the time-averaged MN acceleration:

$$\bar{\mathcal{A}}_x = -\frac{x}{2Ma^2} \{ |E_0|^2 \operatorname{Re} \alpha_{\perp} + |\mathbf{E}_0 \mathbf{n}|^2 \operatorname{Re} (\alpha_{\parallel} - \alpha_{\perp}) \}, \quad (24)$$

$$\bar{\mathcal{A}}_z = \frac{k}{2M} \{ |E_0|^2 \operatorname{Im} \alpha_{\perp} + |\mathbf{E}_0 \mathbf{n}|^2 \operatorname{Im} (\alpha_{\parallel} - \alpha_{\perp}) \}, \quad (25)$$

where  $\mathbf{E}_0^2$  is the density of electromagnetic field. For the linear field polarization along  $y$ -axis, one must change in Eq. (24)  $x$  by  $y$ . Component labeled by  $z$  is along with the spheroid rotation axis and another one labeled by  $x$  (or  $y$ ) is transverse to this axis.

The real and imaginary parts of the polarizability tensor can be written as<sup>16</sup>

$$\operatorname{Re} \alpha_{(\perp)} = \frac{V}{4\pi L_{(\perp)}} \frac{\left( (1 - \xi_m)\omega^2 - \omega_{(\perp)}^2 \right) \left( \omega^2 - \omega_{(\perp)}^2 \right) + \left( 2\omega\gamma_{(\perp)} \right)^2}{\left( \omega^2 - \omega_{(\perp)}^2 \right)^2 + \left( 2\omega\gamma_{(\perp)} \right)^2}, \quad (26)$$

and

$$\operatorname{Im} \alpha_{(\perp)} = \left( \frac{V}{4\pi L_{(\perp)}} \right) \frac{2\omega^3 \xi_m \gamma_{(\perp)}}{\left( \omega^2 - \omega_{(\perp)}^2 \right)^2 + \left( 2\omega\gamma_{(\perp)} \right)^2}, \quad (27)$$

where we have introduced the notations

$$V = \frac{4}{3} \pi R_{\parallel} R_{\perp}^2,$$

$$\xi_m = \frac{\epsilon_m}{\epsilon_m + L_{(\perp)} - L_{(\perp)} \epsilon_m}, \quad (28)$$

$$\omega_{(\perp)}^2 = \frac{L_{(\perp)}}{\epsilon_m + L_{(\perp)} - L_{(\perp)} \epsilon_m} \omega_{pl}^2, \quad (29)$$

and

$$\gamma_{(\perp)} \equiv \gamma_{(\perp)}(\omega) = \frac{2\pi L_{(\perp)}}{\epsilon_m + L_{(\perp)} - L_{(\perp)} \epsilon_m} \sigma_{(\perp)}(\omega) \quad (30)$$

represents the half-width of the resonance  $\alpha$  curve for the light polarized along ( $\parallel$ ) or across ( $\perp$ ) the rotation axis of the spheroid;  $\epsilon_m$  is the dielectric constant of the medium.

For the MN of a spherical form emersed in medium with  $\epsilon_m = 1$ , in the field of the same wave, one get

$$\bar{\mathcal{A}}_{\text{sph}} = \frac{k}{2M} e^{-x^2/a^2} E_0^2 \text{Im } \alpha_{\text{sph}}, \quad (31)$$

$$\bar{\mathcal{A}}_{\text{sph}} = -\frac{x_i}{2Ma^2} e^{-x_i^2/a^2} E_0^2 \text{Re } \alpha_{\text{sph}}, \quad (32)$$

where  $x_i = x, y$  and

$$\text{Re } \alpha_{\text{sph}} = R^3 \frac{(\epsilon' - 1)(\epsilon' + 2) + (4\pi\sigma/\omega)^2}{(\epsilon' + 2)^2 + (4\pi\sigma/\omega)^2}, \quad (33)$$

$$\text{Im } \alpha_{\text{sph}} = R^3 \frac{12\pi\sigma/\omega}{(\epsilon' + 2)^2 + (4\pi\sigma/\omega)^2}, \quad (34)$$

$$\sigma = \frac{3}{16\pi} \frac{v_F}{R} \left( \frac{\omega_{\text{pl}}}{\omega} \right)^2. \quad (35)$$

Here  $R$  is the radius of a spherical MN,  $\sigma$  is its the high-frequency optical conductivity, and we take into account Eq. (10). Expressions (26) and (27), obtained for spheroidal MNs, clearly transforms into the corresponding expressions (33) and (34) for spherical MNs with the account for the equality  $L_{\parallel} = L_{\perp} = 1/3$ . Then the conductivity becomes a scalar quantity, specified in the form (35). At the plasma frequency the real part of the permittivity goes to zero.

Consider now the elliptical polarized Gaussian beam:

$$\mathbf{E}_0 = (\mathbf{b}_1 + i\mathbf{b}_2) e^{-(x^2+y^2)/2a^2} e^{ikz}, \quad (36)$$

$$\mathbf{b}_1 = (b_1, 0, 0), \quad \mathbf{b}_2 = (0, b_2, 0). \quad (37)$$

In this case, after substituting Eqs. (36), (37), and (22) into Eq. (7), we obtain

$$\bar{\mathcal{A}}_i = -\frac{x}{2Ma^2} e^{-(x^2+y^2)/a^2} \{ (b_1^2 + b_2^2) \text{Re } \alpha_{\perp} + [(\mathbf{n}\mathbf{b}_1)^2 + (\mathbf{n}\mathbf{b}_2)^2] \text{Re } (\alpha_{\parallel} - \alpha_{\perp}) \}, \quad (38)$$

with  $i = x, y$ ,

$$\bar{\mathcal{A}}_z = \frac{k}{2M} e^{-(x^2+y^2)/a^2} \{ (b_1^2 + b_2^2) \text{Im } \alpha_{\perp} + [(\mathbf{n}\mathbf{b}_1)^2 + (\mathbf{n}\mathbf{b}_2)^2] \text{Im } (\alpha_{\parallel} - \alpha_{\perp}) \}. \quad (39)$$

One should bear in mind that  $\mathbf{n}$  is a unit vector directed along the rotation axis of the ellipsoid. We see that in this case, the acceleration depends on two angles – between vectors  $\mathbf{n}$  and  $\mathbf{b}_1$  and between  $\mathbf{n}$  and  $\mathbf{b}_2$  ones.

If the components of the unit vector, appearing in Eq. (22), in a spherical coordinate system are represented as

$$n_x = \sin \theta \cos \varphi, \quad n_y = \sin \theta \sin \varphi, \quad n_z = \cos \theta, \quad (40)$$

then the products  $\mathbf{n}\mathbf{b}_1$  and  $\mathbf{n}\mathbf{b}_2$  in Eqs. (38) and (39), respectively, become

$$\mathbf{n}\mathbf{b}_1 = b_1 \sin \theta \cos \varphi, \quad \mathbf{n}\mathbf{b}_2 = b_2 \sin \theta \sin \varphi. \quad (41)$$

In this case the ratio of the average values of the MN acceleration, having spheroidal and spherical forms in the direction of incidence of the radiation can be written, using Eqs. (39) and (31), as follows

$$\frac{\bar{\mathcal{A}}_z}{\bar{\mathcal{A}}_z|_{\text{sph}}} = \frac{\text{Im } \alpha_{\perp}}{\text{Im } \alpha_{\text{sph}}} + \sin^2 \theta \frac{(b_1 \cos \varphi)^2 + (b_2 \sin \varphi)^2}{b_1^2 + b_2^2} \frac{\text{Im } (\alpha_{\parallel} - \alpha_{\perp})}{\text{Im } \alpha_{\text{sph}}}. \quad (42)$$

From Eq. (42), one can see that, contrary to the MNs with a spherical form (when  $\alpha_{\perp} = \alpha_{\parallel}$ ), the acceleration components for the MNs with the ellipsoid-of-revolution geometry acquire the dependence on the angle between the field direction and the revolution axis of a spheroid. In addition, these acceleration components depend on the MN's shape itself, which is determined by the depolarization factors  $L_j$  included in the diagonal components of the tensor  $\alpha_{jj}$ . An analogous relation one can obtained as well for the ratio of the conservative acceleration components  $A_i$  if the imaginary parts of  $\alpha$  in Eq. (42) will be replaced by they real parts.

In the case of circular polarization,  $\mathbf{b}_1 = \mathbf{b}_2 = \mathbf{b}$ , so that

$$(\mathbf{n}\mathbf{b}_1)^2 + (\mathbf{n}\mathbf{b}_2)^2 = (n_x^2 + n_y^2)b^2 = (1 - n_z^2)b^2. \quad (43)$$

That is, in this case, only the dependence on the angle between the vector  $\mathbf{n}$  and the direction of beam propagation survives.

Thus, similarly to the cases of plane-polarized and circularly polarized light beams, the time-averaged acceleration of non-spherical MN becomes angle-dependent. In addition, this acceleration depends on the MN's shape through the components  $\alpha_{\perp}$  and  $\alpha_{\parallel}$  of the polarization tensor; this dependence manifests itself to the maximal extent in the infra-red range of the spectrum (in the vicinity of the CO<sub>2</sub>-laser frequency). For example, taking  $\omega_{\text{pl}} \approx 8 \times 10^{15} \text{ s}^{-1}$  for gold and  $\omega = 2 \times 10^{14} \text{ s}^{-1}$  for the CO<sub>2</sub>-laser frequency, we obtain  $\epsilon' \approx -1600$ . Therefore, the products  $L_{\perp, \parallel}(\epsilon_{\perp, \parallel} - 1)$  that enter into the denominators of formula (16) or (17) are approximately equal

$$L_{\parallel, \perp}(\epsilon_{\parallel, \perp} - 1) \approx -1600 L_{\parallel, \perp}. \quad (44)$$

Since the quantities  $L_{\parallel}$  and  $L_{\perp}$  may vary from 0 to 1 (provided that  $2L_{\perp} + L_{\parallel} = 1$ ), it is clear to which extent quantity (24) and, respectively, the quantities  $\alpha_{\perp}$  and  $\alpha_{\parallel}$  can be sensitive to the form of MN within this range of frequencies.

#### IV. ACCELERATION DUE TO PLASMON RESONANCE

From Eqs. (26) and (27) it is easy to determine the real and imaginary parts of  $\alpha_{\parallel,\perp}$  at resonance frequencies

$$\text{Re } \alpha_{\parallel,\perp} = \frac{V}{4\pi L_{\parallel,\perp}}, \quad \text{Im } \alpha_{\parallel,\perp} = \frac{V}{(4\pi L_{\parallel,\perp})^2} \frac{\omega_{\parallel,\perp}}{\sigma_{\parallel,\perp}}. \quad (45)$$

For a predetermined frequency one can always choose a geometric form of the MN such that it will experience a resonant increase of the acceleration with light pressure. In particular, for MNs of spheroidal shape there exist two form of the spheroid which can resonantly absorb radiation. The opposite statement is also true: MN of an arbitrary geometric shape will absorb resonantly at least one frequency. The higher is the degree of symmetry of the MN, the smaller is the number of resonant frequencies that it can absorb. For example, a spherical MN has one, a spheroidal MN – two, and an ellipsoidal MN – three resonant frequencies.

As one can see from Eq. (42), the value of the MN acceleration ratio depends on both the angle of light incidence  $\theta$  and the light polarization angle  $\varphi$ . Studies have shown that this ratio reaches a maximum value at the angle of incidence equal to  $\theta = \pi/2$ . Setting in Eq. (42) the angle  $\theta$  equal to  $\pi/2$ , let us investigate here how this relation changes for different polarizations of the incident Gaussian beam with a change in the shape of the MN. As an example, select the Cu nanoparticle.

Fig. 1 illustrate the ratio of the acceleration of spheroidal Cu nanoparticle to the acceleration of spherical Cu nanoparticle under light pressure acting in the direction of incidence of the laser beam, as a function of the deviation of the shape of the MN from spherical one. The frequency of laser beam was chosen as  $\omega = 2.9 \times 10^{15} \text{ s}^{-1}$ , which is close to the plasmon modes in copper and  $\epsilon_m = 1$ . As one can see, the resonant acceleration at that frequency is experienced by MNs close to the spherical shape.

Fig. 2 shows the same dependence for the laterally directed pressures. Here and below the calculation of acceleration components are done using Eq. (42), as well as with using the analogous expression obtained with the replacement  $\text{Im} \rightarrow \text{Re}$  for the  $i$ -th pressure.

As is seen in Fig. 1, the acceleration under laser radiation pressure on the Cu nanoparticle in the direction of incidence of the laser beam at the plasmon resonance can be hundreds of times greater than the pressure experienced by a spherical Cu nanoparticle of equal volume.

In the lateral directions (Fig. 2) this excess is much less, not exceeding of tens of times. In this case, the accelerations ratio can be both positive or a negative value that speaks for the attractive or repulsive nature of the pressure (the "radiation wind") acting on MN in these direction. It reaches the maximum in absolute value at angle  $\varphi = \pi/2$ .

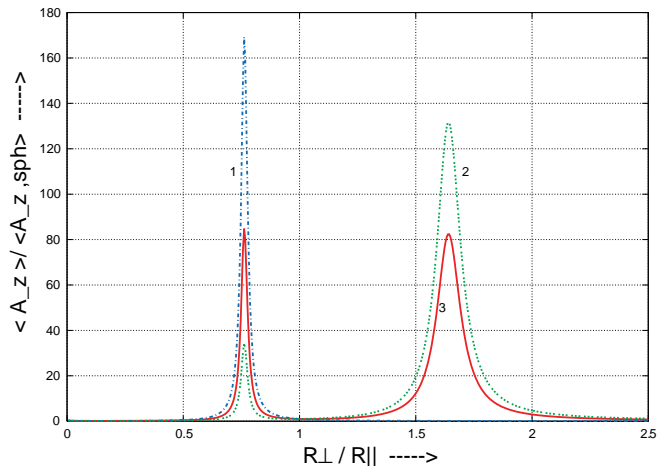


FIG. 1. (Color online) The ratio of the acceleration of spheroidal Cu nanoparticle to acceleration of spherical Cu nanoparticle of equal volume with a radius of  $100\text{\AA}$ , as a function of the Cu shape, in the direction of action of laser beam with frequency  $\omega \simeq 2.9 \cdot 10^{15} \text{ s}^{-1}$  for different polarization: curve 1 (short-dashed line) corresponds to the linear polarization; curve 2 (long-dashed line) corresponds to the elliptical polarization with  $b_1/b_2 = 1/2$ ; curve 3 (solid line) corresponds to the circular polarization.

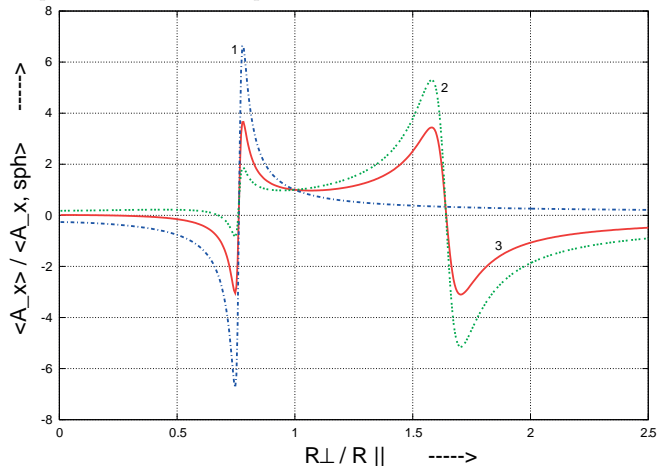


FIG. 2. (Color online) The same as in Fig. 1 for the lateral  $x$ -direction of action of laser beam.

With increasing frequency of the incident radiation, the plasmon resonance occurs for prolate MNs with a greater ratio of  $R_{\perp}/R_{\parallel}$ , while for oblate MNs – with a smaller values of  $R_{\perp}/R_{\parallel}$ . In the last case the pressure forces on the MN fall off in absolute value.

It is also seen (Fig. 2) that in the lateral directions together with the resonance for prolate MNs there is also a resonance for oblate MNs. For low degrees of oblateness this resonance is not suppressed by attenuation as it would be in the case at  $\text{CO}_2$ -laser frequency. In the direction of incidence of the radiation (along the  $z$  axis, Fig. 1), the resonances appear in the form of peaks lying on each side from the spherical shape  $R_{\perp}/R_{\parallel}=1$ .

At the pointed above plasmon frequency for Cu, the resonance acceleration will be manifest itself (in accordance with Eqs. (29) and (13)) both for prolate and oblate MNs with the following values of the ratio  $R_{\perp}/R_{\parallel} = 0.763$ , and  $R_{\perp}/R_{\parallel} = 1.64$ , respectively.

Consequently, the left-hand peak (Fig. 1) and resonance (Fig. 2) pertain to the prolate MN, while the right-hand peak and resonance belong to the oblate MN.

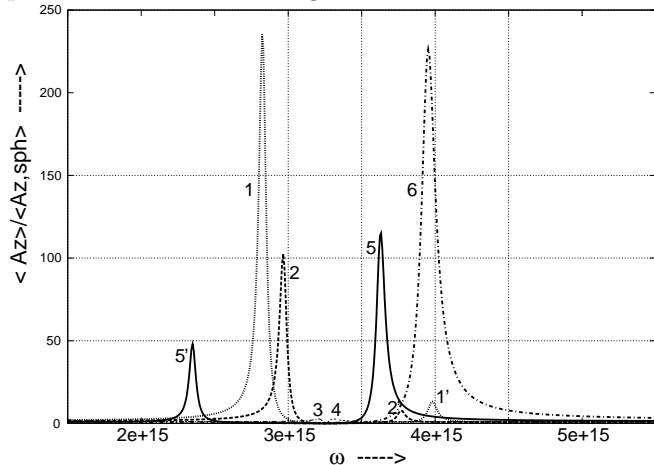


FIG. 3. Frequency dependence of the ratio of MN accelerations in the direction of incidence laser beam for a spheroidal MN to the acceleration of the spherical MN of equal volume with the radius of 100 Å, for nanoparticles with different  $R_{\perp}/R_{\parallel}$ : 1.8(1), 1.5(2), 1.05(3), 0.95(4), 0.5(5), 0.1(6).  $\varphi = \pi/4$ ,  $\theta = \pi/12$ .  $\epsilon_m = 1$ .

As the angle  $\theta$  decreases (with a fixed angle  $\varphi$ ), the resonance peaks in the prolate MN are suppressed, whereas for the oblate MN they reach maximum values. For predetermined orientation (i.e., fixed  $\varphi$  and  $\theta$ ), enhancement or suppression of the resonance peaks in MNs of different shapes can be achieved by selecting the polarization of the incident radiation<sup>17</sup>.

As the MN shape changes, there a shift of the plasmon peaks of the acceleration occurs. To elucidate the nature of these shifts with change in the degree of oblateness or prolateness of the MN, in Fig. 3 we have plotted the frequency dependence of the ratio of MN accelerations with different shapes at fixed angles. The weak peaks 3 and 4 in this figure pertain to the MNs which are close to spherical in shape.

As can be seen from Fig. 3, the oblate MNs manifest resonant acceleration at longer wavelengths (curves 1,2) in comparison with a spherical MN, and the prolate MNs – at shorter wavelengths (curves 5,6). Here the tails of the peaks of the oblate MNs extend toward the long-wavelength side of the spectrum, while those of the prolate MNs extend toward the short-wavelength side. As the flatness of the MN increases (curve 1), the particle acceleration peak increases in absolute value and shifts to the longer wavelengths, while with increasing in elongation of the MN (curve 6) there is, in addition to increase its acceleration, the shift of the peak to the shorter wave-

lengths of the spectrum.

The peaks labeled by numbers with a prime in Fig. 3 arise together with the peaks labeled with the corresponding unprimed numbers; as can be seen from Eq. (29), this is due to their falling into a given range of  $R_{\perp}/R_{\parallel}$  values. Their intensity depends on two factors: the orientation of the MN with respect to the incident radiation and/or polarization of the radiation. In the given example the height of the primed peaks can be controlled by means of the angle  $\theta$ ; they disappear when  $\theta \rightarrow 0$ .

It should be noted that for prolate MNs, the growth of intensity and the peak displacement with an increase in the prolateness of the MN goes to saturation, after which further increase in the prolateness leads to a drop in the intensity of radiation pressure on the MN, and the peak displacement does not occur. The evaluations show that already for  $R_{\perp}/R_{\parallel}=1/64$ , the peak becomes rather wide, and its displacement is not very noticeable in comparison with that for  $R_{\perp}/R_{\parallel}=1/32$ , for example.

## V. CONCLUSION

We have obtained the simple analytical expressions for the acceleration of the spheroidal MN which is exerted by a laser beam averaged over a period of the incident wave. It is shown that the acceleration components can substantially depend on the shape of the MN as well as on the angles that define its orientation both relative to the direction of the incident radiation and to the polarization of the beam.

The behavior of the MN acceleration near plasmon resonances in spheroidal MNs was also investigated, depending on the change in the shape of MN and its orientation. The shift of the resonance peak of the acceleration to longer wavelengths of the spectrum is detected for more oblate MNs and to shorter wavelengths – for more prolate ones. We have established that the value of the accelerations under laser beam action on spheroidal MN can differ by orders of magnitude from the accelerations of the spherical MN of the same volume.

## Acknowledgments

Author is grateful to the Program of the Fundamental Research of the Department of Physics and Astronomy of the National Academy of Sciences of Ukraine (NASU) (0120U100858) for financial support of this work.

<sup>1</sup> T. Iida and H. Ishihara, Phys. Rev. Lett., **90**, 057403 (2003).

<sup>2</sup> M. Perner, S. Gresillon, J. März, G. von Plessen, J. Feldmann, J. Porstendorfer, K.-J. Berg, and G. Berg, Phys.

Rev. Lett., **85**, 792 (2000).

<sup>3</sup> R. Gómez-Medina, P. San José, A. Garcia-Martin, M. Lester, M. Nieto-Vesperinas, & J.J. Sáenz, Phys. Rev. Lett., **86**, 4275 (2001).

- <sup>4</sup> E.G. Rawson and A.D. May, Appl. Phys. Lett., **8**, 93 (1966).
- <sup>5</sup> A. Ashkin, Phys. Rev. Lett., **24**, 156 (1970).
- <sup>6</sup> A. Ashkin, J.M. Dziedzic, Phys. Rev. Lett., **38**, 1351 (1977).
- <sup>7</sup> J.R. Arias-González, and M. Nieto-Vesperinas, J. Opt. Soc. Am. A, **20**, 1201 (2003).
- <sup>8</sup> L. Novotny, R.X. Bian, and X.S. Xie, Phys. Rev. Lett., **79**, 645 (1997).
- <sup>9</sup> P.C. Chaumet, A. Rahmani, and M. Nieto-Vesperinas, Phys. Rev. B., **71**, 045425 (2005).
- <sup>10</sup> N.I. Grigorchuk, JOSA B, **35**, 2851 (2018).
- <sup>11</sup> N. Song, R. Li, H. Sun, J. Zhang, B. Wei, S. Zhang, and F.G. Mitri, J. Quant. Spectrosc. Radiat. Transfer, **245**, 106853 (2020).
- <sup>12</sup> S. Sukhov, A. Dogariu, Rep. Prog. Phys., **80**, 112001 (2017).
- <sup>13</sup> P.M. Tomchuk and N.I. Grigorchuk, Phys. Rev. B, **73**, 155423 (2006).
- <sup>14</sup> N.I. Grigorchuk, Eur. Phys. Lett., **121**, 67003 (2018).
- <sup>15</sup> C.F. Bohren and D.R. Huffman, *Absorption and Scattering of Light by Small Particles* (Wiley, Weinheim, 2004).
- <sup>16</sup> N.I. Grigorchuk, Eur. Phys. Lett., **97**, 45001 (2012).
- <sup>17</sup> H. Kimura, I. Mann, Quant. Spectrosc. Radiat. Transfer, **60**, 425 (1998).